

## Distinctive features of tumor-infiltrating $\gamma\delta$ T lymphocytes in human colorectal cancer

S. Meraviglia, E. Lo Presti, M. Tosolini, C. La Mendola, V. Orlando, M. Todaro, V. Catalano, G. Stassi, G. Cicero, S. Vieni, J. J. Fourniè & F. Dieli

To cite this article: S. Meraviglia, E. Lo Presti, M. Tosolini, C. La Mendola, V. Orlando, M. Todaro, V. Catalano, G. Stassi, G. Cicero, S. Vieni, J. J. Fourniè & F. Dieli (2017): Distinctive features of tumor-infiltrating  $\gamma\delta$  T lymphocytes in human colorectal cancer, Oncoimmunology, DOI: [10.1080/2162402X.2017.1347742](https://doi.org/10.1080/2162402X.2017.1347742)

To link to this article: <http://dx.doi.org/10.1080/2162402X.2017.1347742>



Accepted author version posted online: 13 Jul 2017.  
Published online: 13 Jul 2017.



Submit your article to this journal [↗](#)



Article views: 28



View related articles [↗](#)



View Crossmark data [↗](#)

ORIGINAL RESEARCH



## Distinctive features of tumor-infiltrating $\gamma\delta$ T lymphocytes in human colorectal cancer

S. Meraviglia<sup>a,b</sup>, E. Lo Presti<sup>a,b</sup>, M. Tosolini<sup>ibc</sup>, C. La Mendola<sup>a,b</sup>, V. Orlando<sup>a,b</sup>, M. Todaro<sup>a,d</sup>, V. Catalano<sup>a</sup>, G. Stassi<sup>e</sup>, G. Cicero<sup>e</sup>, S. Vieni<sup>e</sup>, J. J. Fourniè<sup>idc</sup>, and F. Dielli<sup>a,b</sup>

<sup>a</sup>Central Laboratory of Advanced Diagnosis and Biomedical Research (CLADIBIOR), University of Palermo, Palermo, Italy; <sup>b</sup>Department of Biopathology and Medical Biotechnologies (DIBIMED), University of Palermo, Palermo, Italy; <sup>c</sup>Centre de Recherches en Cancérologie de Toulouse (CRCT), Toulouse, France; <sup>d</sup>Department of Medicine, University of Palermo, Palermo, Italy; <sup>e</sup>Department of Surgical and Oncological Sciences, University of Palermo, Palermo, Italy

### ABSTRACT

$\gamma\delta$  T cells usually infiltrate many different types of cancer, but it is unclear whether they inhibit or promote tumor progression. Moreover, properties of tumor-infiltrating  $\gamma\delta$  T cells and those in the corresponding normal tissue remain largely unknown. Here we have studied features of  $\gamma\delta$  T cells in colorectal cancer, normal colon tissue and peripheral blood, and correlated their levels with clinicopathologic hallmarks. Flow cytometry and transcriptome analyses showed that the tumor comprised a highly variable rate of TILs (5–90%) and 4%  $\gamma\delta$  T cells on average, with the majority expressing V $\delta$ 1. Most V $\delta$ 1 and V $\delta$ 2 T cells showed a predominant effector memory phenotype and had reduced production of IFN- $\gamma$  which was likely due to yet unidentified inhibitory molecules present in cancer stem cell secretome. Transcriptome analyses revealed that patients containing abundant  $\gamma\delta$  T cells had significantly longer 5-year disease free survival rate, suggesting their efficacy in controlling tumor at very early stage.

### ARTICLE HISTORY

Received 31 March 2017  
Revised 14 June 2017  
Accepted 22 June 2017

### KEYWORDS

$\gamma\delta$  T cells; colon cancer; DFS; IFN- $\gamma$ ; TILs

### Introduction

Colorectal cancer (CRC) is one of the top 3 causes of cancer death.<sup>1–4</sup> CRC arises from the inner wall of the large intestine and results from the accumulation of diverse genomic aberrations. These include both inherited mutations causing hereditary CRC<sup>5</sup> and several chromosomal locations and single nucleotide polymorphisms (SNPs) which confer increased risk for CRC development. Moreover, tumor cells grow in a very complex microenvironment and establish reciprocal interactions with epithelial and mesenchymal cells, vascular and lymphatic vessels, inflammatory and immune cells.<sup>6–8</sup>

Tumor-infiltrating lymphocytes (TILs) are an immune population composed of different immune cells that have specificity and potential reactivity against the tumor. TILs have been found in a wide variety of solid tumors including CRC.<sup>9–10</sup> However, while the functions and anti-CRC activities of CD4 and CD8 T cells within TILs have been extensively studied,<sup>11–12</sup> very little is known about  $\gamma\delta$  T lymphocytes.

$\gamma\delta$  T lymphocytes are important effector cells of the immune system that may play a role in the anti-tumor immunosurveillance. Human  $\gamma\delta$  T cells can be divided into 2 main populations based upon  $\delta$  chain expression<sup>13</sup>:  $\gamma\delta$  T cells expressing the V $\delta$ 1 chain are mostly found in mucosal tissues, while  $\gamma\delta$  T cells expressing the V $\delta$ 2 chain (preferentially paired to the V $\gamma$ 9 chain) predominate in the peripheral blood and secondary lymphoid organs.<sup>14</sup> While the ligand(s) recognized by V $\delta$ 1 cells

remain unknown, V $\delta$ 2 T cells recognize non peptidic Ags by a MHC-unrestricted mechanism,<sup>15–17</sup> but which involves butyrophilin (BTN) 3A1.<sup>18–20</sup> Specifically, V $\gamma$ 9V $\delta$ 2 T cells recognize small unprocessed non peptidic compounds containing phosphate and termed phosphoantigens (PAGs), that are produced through the isoprenoid biosynthesis pathway.<sup>15–17</sup> Moreover, these cells can also be activated, through an indirect mechanism, by aminobisphosphonates that inhibit farnesyl pyrophosphate synthase and cause accumulation of downstream endogenous PAGs.<sup>21–22</sup> Physiologic levels of PAGs, however, are not stimulatory of V $\gamma$ 9V $\delta$ 2 T cells, but transformed and infected cells would produce increased metabolic intermediates such as PAGs. Upon activation,  $\gamma\delta$  T lymphocytes undergo a differentiation program resembling that of CD8 T cells and they give rise to both central memory ( $T_{CM}$ ; CD45RA<sup>−</sup> CD27<sup>+</sup>) and effector memory ( $T_{EM}$ ; CD45RA<sup>−</sup> CD27<sup>−</sup>) and terminally differentiated ( $T_{EMRA}$ ; CD45RA<sup>+</sup> CD27<sup>−</sup>) T cells.  $\gamma\delta$   $T_{CM}$  cells home to secondary lymphoid organs and lack immediate effector functions, while  $\gamma\delta$   $T_{EM}$  and  $T_{EMRA}$  cells home to sites of inflammation where they display immediate effector functions such as cytokine production and cytotoxicity, respectively.<sup>23</sup> Based on their effector properties, V $\gamma$ 9V $\delta$ 2 T lymphocytes are supposed to play an important role in cellular immune responses against tumors.

$\gamma\delta$  T cells have been found among TILs in many different types of cancer, but it is unclear if they correlate positively or

not with tumor growth, or even fail to correlate with any prognostic feature.<sup>24-25</sup> With particular regard to CRC,  $\gamma\delta$  T cells among TILs are the major source of IL-17 and positively correlate with advanced tumor clinicopathologic features.<sup>26</sup> However, a very recent analysis of expression signature from ~18,000 human tumors with overall survival outcomes across a collection of 39 cancer types, including CRC, revealed intratumoral  $\gamma\delta$  cells as the most significant favorable prognostic immune population.<sup>27</sup> Therefore, there is urgent need to revisit and clarify this issue and also to understand the reciprocal interactions between  $\gamma\delta$  cells and other components of the tumor microenvironment, because these interactions can influence the function of intratumoral  $\gamma\delta$  cells and thus the net outcome of their response to tumor.

In this paper, we have studied the frequency, phenotype and functions of  $\gamma\delta$  T cells infiltrating CRC and correlated levels of intratumoral  $\gamma\delta$  T cells with clinical outcome. Moreover, we have studied the influence of the tumor microenvironment on the functional responses of  $\gamma\delta$  T cells.

## Results

### $\gamma\delta$ T cells are present among CRC TILs

To evaluate the composition of tumor-infiltrating leukocytes in human CRC, CRC tissues were freshly obtained from 70 patients undergoing surgery, and analysis of cell surface

molecules defining T, B, NK cells and  $\gamma\delta$  T cells was performed using polychromatic flow cytometry. Cumulative data are shown in Fig. 1a. Immune infiltrates detected with the pan-leukocyte marker CD45 were present in both normal and tumor tissues, but were substantially increased in CRC compared with normal tissue (CRC: median = 68%, range 15–87.8%; Healthy tissue: median = 61%, range 33.9–85%). Lymphocyte subsets were evaluated by the use of cell-surface markers and indicated as percentage of the total number of CD45<sup>+</sup> cells in each sample (Fig. 1a). CD3<sup>+</sup> T cells represented an average of 20% of the whole leukocyte (CD45<sup>+</sup>) population within the analyzed primary CRC samples, and consisted mainly of CD4<sup>+</sup> and CD8<sup>+</sup> T cells, each of which accounted for 8% of the CD45<sup>+</sup> population (hence each accounting for 40% of the CD3<sup>+</sup> population). Percentages of B and NK lymphocytes were lower than percentages of CD3<sup>+</sup> cells (6% for CD3<sup>-</sup> CD19<sup>+</sup> cells and 10% for CD3<sup>-</sup> CD56<sup>+</sup> cells).  $\gamma\delta$  T cells were present among intratumoral leukocytes and accounted for approximately 4.5% (mean 4.5%  $\pm$  4.9%) of the total leukocyte population (Fig. 1a), hence accounting for approximately 20% of the CD3<sup>+</sup> population. For comparison, we data mined an independent cohort of 585 CRC transcriptomes<sup>28</sup> acquired on Affymetrix U133plus2 microarrays and downloaded from the NCBI-GEO data set repository.<sup>29</sup> The algorithmic deconvolution of leucocytes infiltrating these tumors by CIBERSORT-LM7<sup>30-31</sup> detected on average 4.9%  $\pm$  4.4%  $\gamma\delta$  TILs among the total leucocyte population in these samples. Hence the above FACS results were

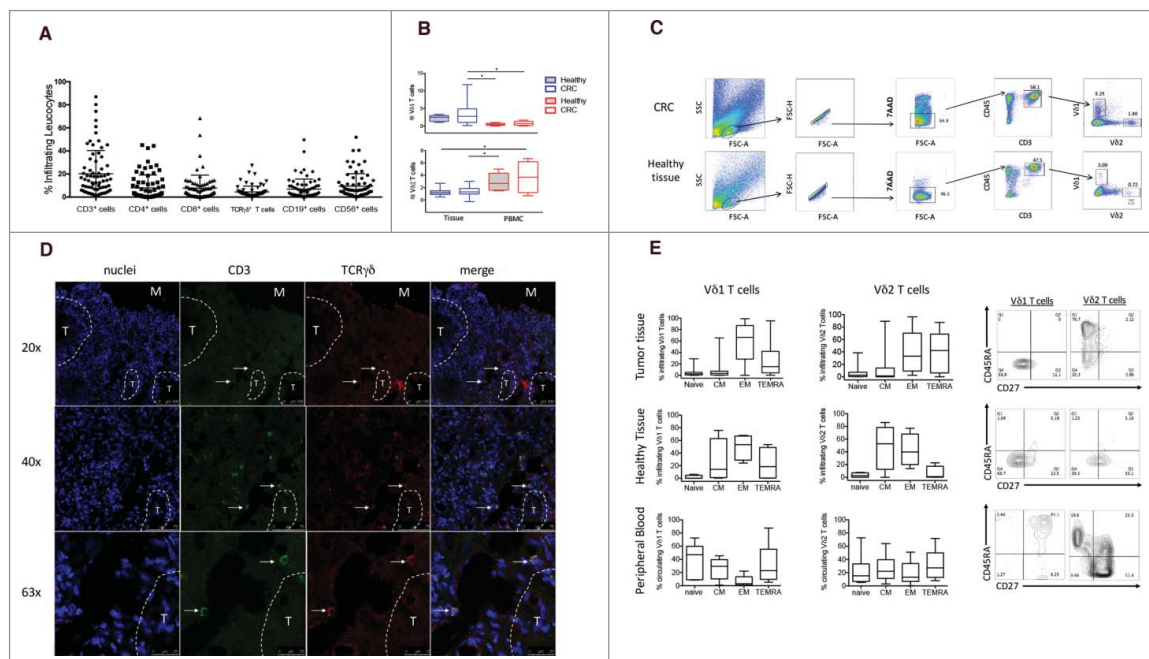


**Figure 1.** Frequency of infiltrating and circulating  $\gamma\delta$  T cells expressing either V $\delta$ 1 or V $\delta$ 2 TCR  $\delta$  chains in HD and CRC patients. (A) Cumulative analysis of immune infiltrates of 70 colon cancer specimens. Lymphomonocyte populations were evaluated by the use of cell-surface markers and indicated as percentage of the total number of CD45<sup>+</sup> cells in each sample. (B) Box plot of percentages of V $\delta$ 1 or V $\delta$ 2  $\gamma\delta$  T cells subsets in healthy tissue, tumor tissue and peripheral blood of CRC patients and peripheral blood of HD subjects. Boxes represent 25th to 75th percentiles; middle bar identifies median; whiskers show minimum and maximum. \* $p < 0.05$  performed by non-parametric Mann-Whitney test, unpaired and 2-tailed with confidential interval 95%. (C) Representative dot plots of the gating strategy used to define V $\delta$ 1 and V $\delta$ 2 T cells from healthy and tumor tissues. The following gating strategy was used to detect  $\gamma\delta$  T lymphocytes: FSC/SSC, single cells, live cells CD45/CD3, V $\delta$ 1 and V $\delta$ 2 T cells. (D) Sections from CRC patients were stained with anti-human pan- $\gamma\delta$  TCR (red) and anti-CD3 (green) for immunofluorescent (IF) staining. Right panel is a magnified view and the arrows display the colocalization of  $\gamma\delta$  TCR and CD3. Nuclei were contrasted with DAPI. One of 3 independent experiments is shown. (E) Phenotypic analysis of V $\delta$ 1 and V $\delta$ 2 T cells among healthy and tumor tissues and PBMC of CRC patients, upon staining with mAbs to CD45RA and CD27, and gating on CD3<sup>+</sup> V $\delta$ 1<sup>+</sup> or CD3<sup>+</sup> V $\delta$ 2<sup>+</sup> T cells. Beside, flow cytometry panels of a representative dot plot. Isotype-matched mAbs were used as controls. Viable lymphocytes were gated by forward and side scatter, and analysis was performed on 100,000 acquired events by using FlowJo. PBMC were stained with anti-CD3, anti-V $\delta$ 2, anti-CD45RA and CD27 mAbs.

fully consistent with those from an independent cohort of CRC (Wilcoxon  $p$  value = 0.26 for comparison of the 2 series of  $\gamma\delta$  TIL rates). As shown in Fig. 1a, there was an extremely high variability in percentages of lymphocyte subsets detected among TILs in the tested CRC patients. This was strikingly depicted by both the raw FACS data and the microarray deconvolution for percentages of CD3<sup>+</sup> T cells which ranged between 5% to 90% (FACS) and 4% to 70% (microarrays).

$\gamma\delta$  T cells variably infiltrate several human cancers, but the current data on the prognostic value of intratumoral  $\gamma\delta$  T cells have shown marked variability.<sup>27</sup> To study whether this was dependent on the prevalence of a given  $\gamma\delta$  subset among TILs, we evaluated V $\delta$ 1 and V $\delta$ 2 T cells from CRC and adjacent non tumor colon tissue to determine their frequencies and composition. Fig. 1b shows cumulative data from 70 CRC patients, while Fig. 1c shows primary data from one representative sample per each group. As compared with adjacent non tumor colon tissue, intratumoral  $\gamma\delta$  T cells did not exhibit a distinct

prevalence and distribution of V $\delta$ 1 and V $\delta$ 2 T cell subsets, despite a slightly and not significantly increased abundance of both subsets (Fig. 1b). As expected, the majority of  $\gamma\delta$  T cells in both CRC and adjacent normal tissues expressed V $\delta$ 1, and this pattern was observed in multiple patients despite the frequencies of V $\delta$ 1 and V $\delta$ 2 T cells among tumor-infiltrating leukocytes varied widely. This TCR bias could not be investigated likewise using the microarray data set which lacks *TRDV1* gene, and in which the correlated levels of *TRGV9* and *TRDV2* genes indicated presence of TCR V $\gamma$ 9V $\delta$ 2 T lymphocytes (data not shown).

Because previous papers<sup>11-12</sup> have emphasized the importance of immune cell localization, within distinct tumor regions, related to the risk of tumor recurrence, we also visualized intratumoral  $\gamma\delta$  T cells by immunofluorescence analysis on frozen sections. In our analysis,  $\gamma\delta$  T cells were consistently detected in the tumor border/stroma, but only very rarely in the intratumor tissue (Fig. 1d).

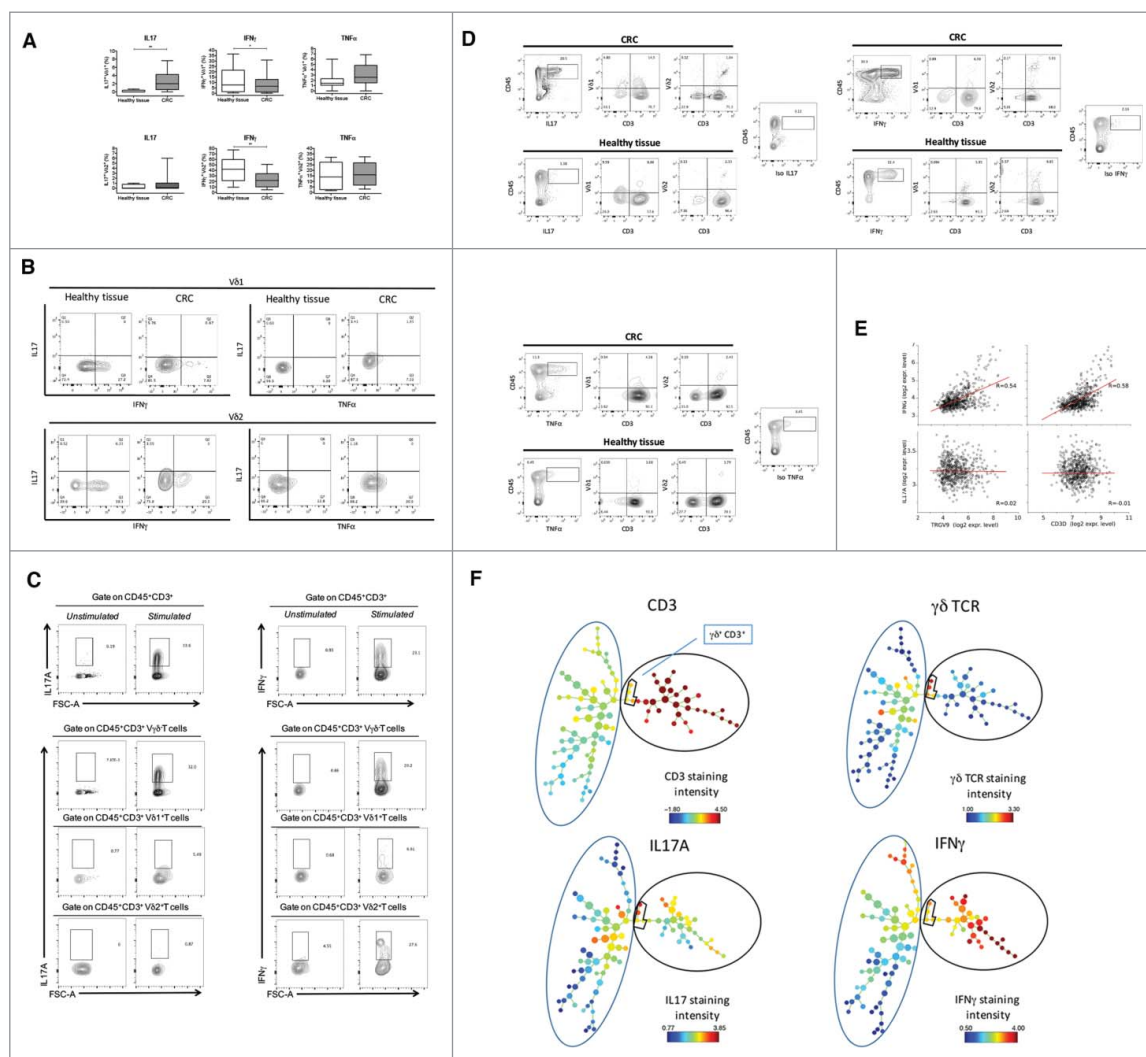


**Figure 2.** Cytokine production of tumor infiltrating  $\gamma\delta$  T cells. (A) Box plots of cumulative data of healthy tissue and tumor tissue samples from 20 CRC patients. Cells were stimulated *in vitro* as described in Materials and Methods and were stained with mAbs to IFN- $\gamma$ , IL-17 and TNF- $\alpha$ . \* $p$ <0.05 and \*\* $p$ <0.01 performed by nonparametric Mann-Whitney test, unpaired and 2-tailed with confidential interval 95%. (B) Flow cytometry analysis of healthy and tumor tissue from one representative CRC patient. (C) Representative dot plots to define IL-17 or IFN- $\gamma$  producing  $\gamma\delta$ , V $\delta$ 1 and V $\delta$ 2 T cells gated separately on CD45<sup>+</sup>CD3<sup>+</sup> $\gamma\delta$ <sup>+</sup>, CD45<sup>+</sup>CD3<sup>+</sup>V $\delta$ 1<sup>+</sup> or CD45<sup>+</sup>CD3<sup>+</sup>V $\delta$ 2<sup>+</sup> T cells. (D) Representative dot plots to define cells making IL-17 or IFN- $\gamma$  upon gating on CD45<sup>+</sup>IL-17<sup>+</sup> or CD45<sup>+</sup>IFN- $\gamma$ <sup>+</sup> cells, of healthy and tumor tissue. (E) Pearson correlation of *TCR*, *IFNG* and *IL17A* gene expression levels in  $n = 585$  CRC tumor samples. \*\* $p$ <0.01. (F) CRC-infiltrating CD45<sup>+</sup> single cells were used to generate the SPADE tree, and were grouped in 2 different populations, CD3<sup>-</sup> and CD3<sup>+</sup> (black outer circles). The distribution of the major populations is showed for one representative sample. The branching tree is based on the number of cells included in each node and the legend indicates the range of cell per node according to relative median fluorescence intensity.

Most V $\delta$ 1 T cells in tumor tissues were of effector memory phenotype (T<sub>EM</sub>), whereas T<sub>EMRA</sub>, T<sub>Naive</sub> and T<sub>CM</sub> cells accounted for 15%, 3% and 3.5% of the total  $\gamma\delta$  population, respectively (Fig. 1e). Conversely, intratumoral V $\delta$ 2 T cells had a more heterogeneous phenotype with T<sub>EM</sub> and T<sub>EMRA</sub> cells almost equally well represented (33% and 42% respectively) and T<sub>CM</sub> and T<sub>Naive</sub> phenotypes accounting for only 3% and 2% of the total  $\gamma\delta$  population, respectively.

To understand if the predominance of  $\gamma\delta$  T cells with effector phenotypes in TILs was due to the tumor microenvironment or simply reflected an overall bias in colon cancer patients, we compared the phenotype distribution of V $\delta$ 1 and V $\delta$ 2 T cells in the tumor tissue with that in adjacent non tumor colon tissue and in peripheral blood. The cell-surface differentiation patterns of CRC-resident V $\delta$ 1 and V $\delta$ 2 T cells were very similar to those of V $\delta$ 1 and V $\delta$ 2 T cells residing in adjacent non tumor colon tissue, but distinct from those of the corresponding cells from the peripheral blood (Fig. 1e). This indicates that residence in a non-lymphoid tissue, regardless of whether it is normal or has undergone tumor transformation, serves as a major determinant of the phenotypic characteristics of tumor and tissue  $\gamma\delta$  T cells.

### Functional features of CRC-infiltrating $\gamma\delta$ T cells

To further elucidate the functional state of infiltrating  $\gamma\delta$  T cells, we analyzed the production of IL-17, IFN- $\gamma$  and TNF- $\alpha$  by tumor-infiltrating V $\delta$ 1 and V $\delta$ 2 T cells, upon *in vitro* stimulation with ionomycin and PMA. Fig. 2a shows cumulative data from 20 CRC patients and Fig. 2b shows primary data from one representative sample per each group.

Upon activation, V $\delta$ 1 T cells from adjacent non tumor colon tissue produced IFN- $\gamma$ , but very poor, if any, IL-17 and TNF- $\alpha$ . In contrast, V $\delta$ 1 T cells from CRC tissues produced significantly less IFN- $\gamma$  compared with adjacent non tumor colon tissue (8.1% versus 1.2%), but expressed more IL-17 (2.7% vs. 0.2%) and TNF- $\alpha$  (3% vs. 1.9%). Similarly, upon activation V $\delta$ 2 T cells from adjacent non tumor colon tissue expressed both IFN- $\gamma$  and TNF- $\alpha$ , but very low levels IL-17, while V $\delta$ 2 T cells from CRC tissues expressed significantly less IFN- $\gamma$  (23.5% vs. 41.2%) and had similar TNF- $\alpha$  (16.9% vs. 14.6%) and IL-17 expression (1% vs. 0.4%). These results were confirmed by the measurement of IFN- $\gamma$ , IL-17 and TNF- $\alpha$  concentrations in culture supernatants of V $\delta$ 1 and V $\delta$ 2 T cells by ELISA (data not shown). Moreover, the very poor IL-17 production by CRC infiltrating  $\gamma\delta$  T cells was confirmed when we differently gated through more stringent leukocyte gates (CD45<sup>+</sup> CD3<sup>+</sup> $\gamma\delta$ <sup>-</sup>, CD45<sup>+</sup> CD3<sup>+</sup> V $\delta$ 1<sup>+</sup> or CD45<sup>+</sup> CD3<sup>+</sup> V $\delta$ 2<sup>+</sup> T cells): in fact, 5% V $\delta$ 1<sup>+</sup> and 0.87% V $\delta$ 2<sup>+</sup> cells expressed IL-17, and 10% V $\delta$ 1<sup>+</sup> and 27.6% V $\delta$ 2<sup>+</sup> cells expressed IFN- $\gamma$  (Fig. 2c).

The above finding was unexpected, because a previous study has shown that  $\gamma\delta$  T cells are the major cellular source of IL-17 in human CRC.<sup>26</sup> Given that, and to exclude a general failure of IL-17 production in our experimental settings, we used another different strategy: we gated first on IL-17-producing leukocytes (CD45<sup>+</sup> IL-17<sup>+</sup>) and then checked the phenotype of cells making IL-17 among tumor-infiltrating leukocytes. As shown in Fig. 2d the majority of CD45<sup>+</sup> IL-17<sup>+</sup> cells both in CRC and in

adjacent non tumor colon tissues were CD3<sup>+</sup> but did not express either V $\delta$ 1 or V $\delta$ 2, suggesting they may be typical Th17 or Tc17  $\alpha\beta$  T cells. Moreover, a discrete fraction of CD45<sup>+</sup> IL-17<sup>+</sup> cells (ranging from 10% to 50% in different samples), which was increased in CRC tissues as compared with adjacent non tumor colon tissue, did not express CD3 and probably corresponds to type 3 innate lymphoid cells (ILC3) or other leukocyte populations. Using this same gating strategy, we also show that most of cells expressing IFN- $\gamma$  and TNF- $\alpha$  were CD3<sup>+</sup> but V $\delta$ 1<sup>-</sup> and V $\delta$ 2<sup>-</sup> T cells, both in CRC and adjacent non tumor colon tissues.

In the CRC microarray data set as well, expression of *TRGV9*, *TRDV2* or *CD3D* genes was correlated with expression of *IFNG* gene, suggesting that TILs in general and TCRV $\gamma$ 9V $\delta$ 2 cells in particular are involved in producing this cytokine in CRC samples. By contrast such correlations were not found with expression of *IL17A* gene, suggesting that IL-17 production arises from more diverse cell sources than *IFNG* (Fig. 2e). This possibility was also supported by SPADE (Spanning-Tree Progression Analysis of Density-normalized Events) algorithm, which distinguishes cell subsets by clustering, based on surface antigen expression denoted by a color gradient: as shown in Fig. 2f, IFN- $\gamma$  had diverse maps compared with those of IL-17.

Together, these results indicate that V $\delta$ 1 and V $\delta$ 2 T cells in CRC and adjacent normal tissues preferentially produce IFN- $\gamma$ , but very low IL-17, almost as all the other CD3<sup>+</sup> TILs in human CRC. Moreover, IFN- $\gamma$  production by both V $\delta$ 1 and V $\delta$ 2 T cells is significantly reduced in CRC tissues, as compared with adjacent normal colon tissue samples.

### CRC-infiltrating $\gamma\delta$ T cells are largely shaped by the local tumor microenvironment

Next we sought to explore whether the tumor microenvironment imparts distinct functional features on  $\gamma\delta$  T cells. In particular, it is conceivable that tissue resident  $\gamma\delta$  T cells are functionally affected locally or it is also possible that  $\gamma\delta$  T cells are recruited into the tumor from draining lymph nodes or peripheral blood and then undergo functional changes in response to the local microenvironment.

To test the influence of the tumor environment on  $\gamma\delta$  T cells, we initially isolated cancer stem cells (CSC) and cancer-associated fibroblasts (CAF) from 15 CRC patients and tested the effect of the 48-hrs culture supernatants from CSC and CAF on polyclonal  $\gamma\delta$  T cell lines (containing both V $\delta$ 1 and V $\delta$ 2 T cells) obtained from peripheral blood of healthy donors. As shown in Fig. 3a, supernatants from CSC, but not supernatants from CAF significantly impaired proliferation of polyclonal  $\gamma\delta$  T cells to PHA. Supernatants from CSC also inhibited proliferation of polyclonal  $\gamma\delta$  T cells stimulated with anti-CD3 and anti-CD28, or proliferation of V $\delta$ 2 T cells from peripheral blood stimulated with zoledronate + IL-2 in a 7-day culture setting. (data not shown).

Supernatants from CSC were also capable to significantly inhibit IFN- $\gamma$  production by polyclonal  $\gamma\delta$  T cell lines and promoted production of IL-17, while supernatants from CAF only minimally inhibited IFN- $\gamma$  production and did not induce IL-17 production by  $\gamma\delta$  T cell lines (Fig. 3b). Overall, these results indicate that cells in the tumor microenvironment, and

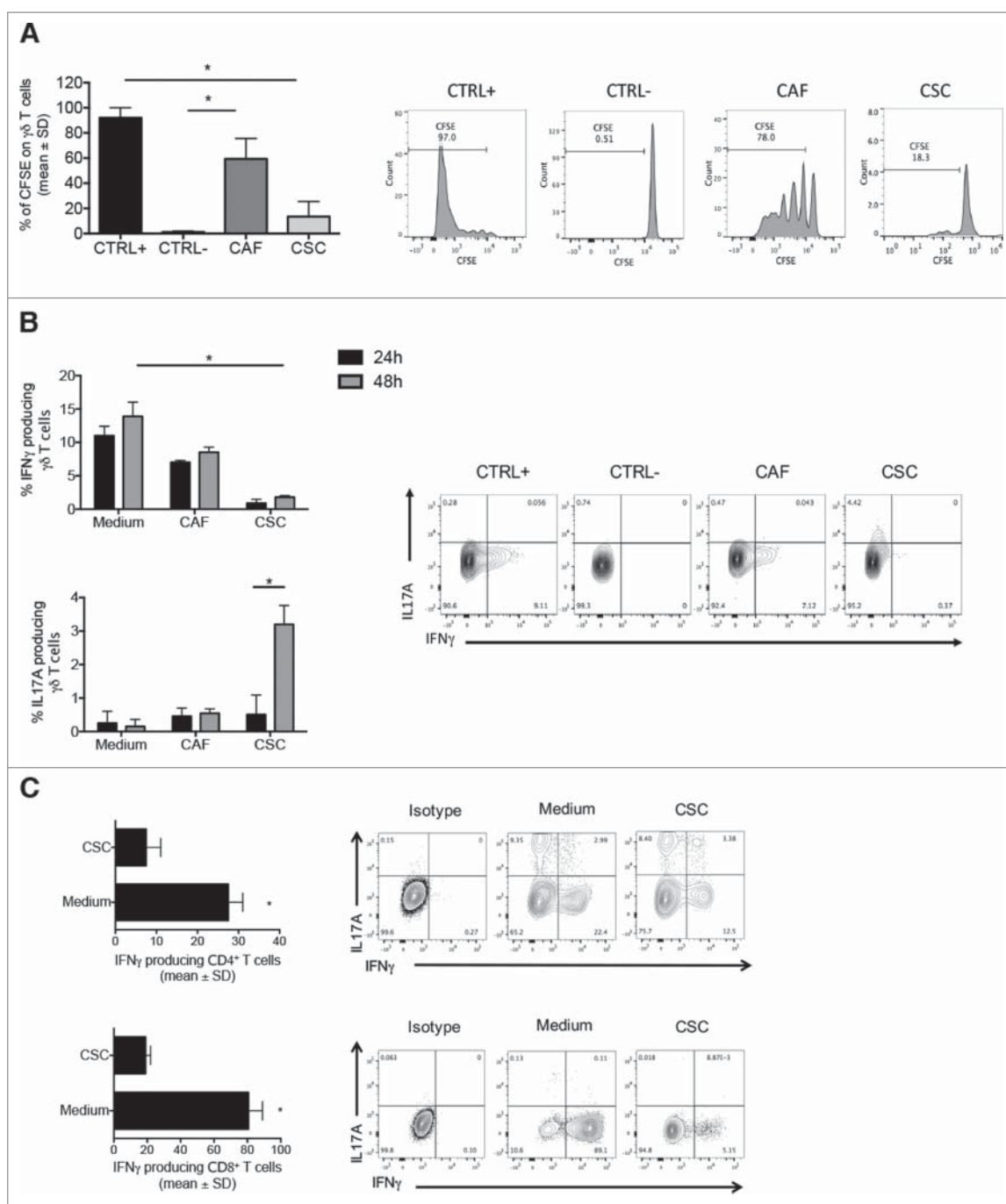


**Figure 3.** CSC supernatants inhibit proliferation and IFN- $\gamma$  production by  $\gamma\delta$ , CD4 and CD8 T cells. (A) Cumulative data ( $n = 5$ ) from proliferation assay. Positive control (CTRL+) and negative control (CTRL-) refer to cells stimulated with PHA and unstimulated cells, respectively. Data are mean percentage of positive cells  $\pm$  SD. Shown also histogram plots of proliferation of  $\gamma\delta$  T cells upon culture with PHA and in the presence of CAF and CSC supernatants. (B) Frequency of IL-17- or IFN- $\gamma$ -producing  $\gamma\delta$  T cells upon incubation for 24 or 48 hrs with PHA in the presence of CAF or CSC supernatant. Histograms show cumulative data from 5 different experiments. Error bars indicate SD. Shown are also representative dot plots. (C) Cumulative and flow cytometry analysis of IFN- $\gamma$  and IL-17 production by CD4 and CD8 T cells upon incubation for 48 hrs with PHA in the presence of CAF or CSC supernatant. \* $p < 0.05$ .

particularly CSC, produce immunomodulatory molecules capable to inhibit proliferation and IFN- $\gamma$  production by  $\gamma\delta$  T cells and to promote their IL-17 production.

To test whether the effect of CSC supernatants was restricted to  $\gamma\delta$  T cells or was rather a more general phenomenon, we generated polyclonal CD4 and CD8  $\alpha\beta$  T cell lines and tested the capability of 48-hrs CSC supernatants to inhibit IFN- $\gamma$  production. As shown in Fig. 3c, supernatants from CSC significantly inhibited IFN- $\gamma$  production by both CD4 and CD8 T

cells lines, thus indicating that inhibitory molecules produced by CSC have a profound effect on several components of both adaptive ( $\alpha\beta$ ) and innate-like ( $\gamma\delta$ ) T cell immune response.

The above reported data clearly demonstrate the presence of biologically important immunomodulatory molecules in CSC secretome. Therefore, we performed a comparative analysis of levels of 50 different cytokines in supernatants of CSC and CAF by the Luminex platform. As shown in Fig. 4a, CSC produced remarkably elevated levels of several cytokines, while

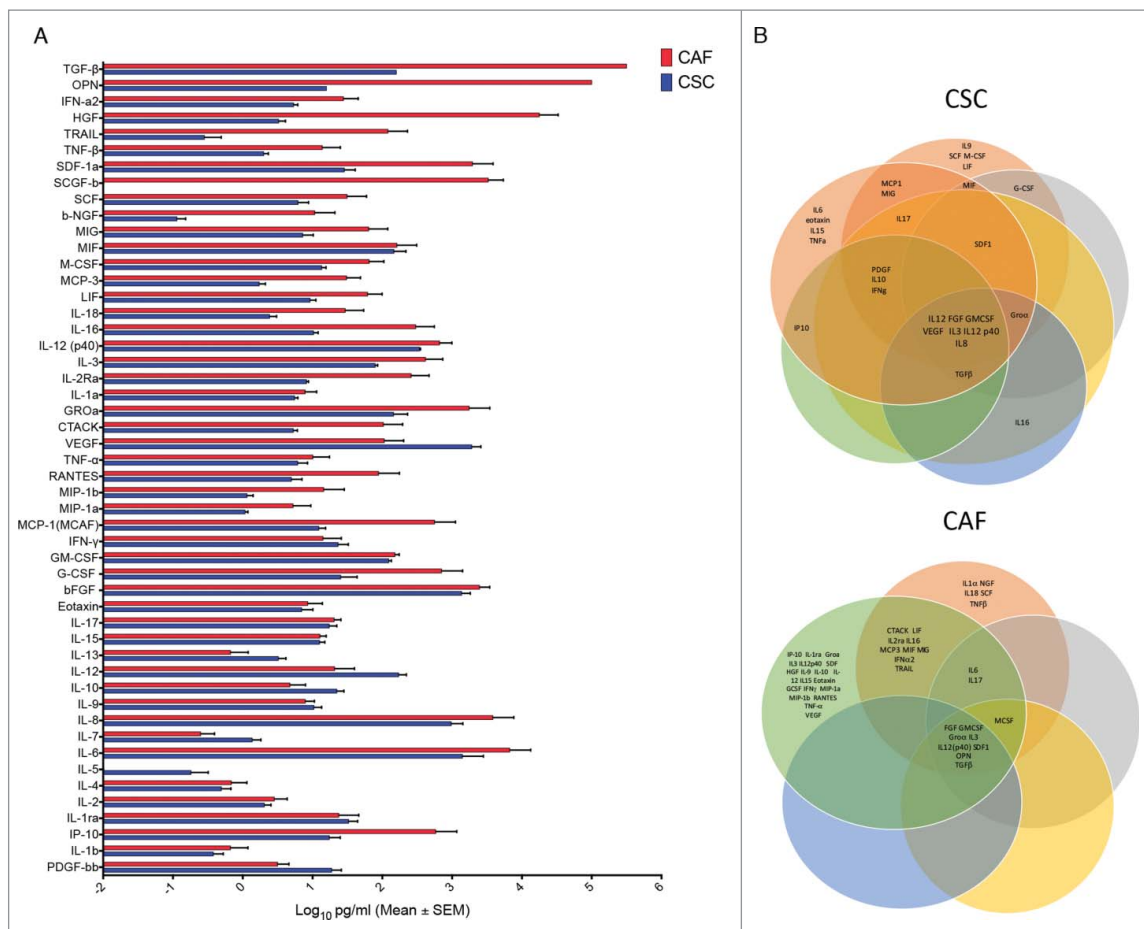


**Figure 4.** Comparative analysis of 50 different cytokines in CSC and CAF secretome (A) Levels of 50 different cytokines in 48 hrs supernatants of CSC and CAF by the Luminox platform. (B) Cytokine grouping in 6 CRC and 5 CAF samples as represented by Venn diagrams.

CAF had a more limited cytokine producing capabilities, with the exception of TGF- $\beta$  which was preferentially produced by CAF. We then checked at cytokines which were differentially expressed in the inhibitory CSC secretome, but not in the non inhibitory CAF secretome. As shown in Fig. 4b, although there were several molecules unique to each CSC or CAF secretome, there were only 8 common molecules to every CSC secretome (FGF, GM-CSF, VEGF, Gro $\alpha$ , IL-3, IL-8, IL-12 and IL-12p40), and 9 common molecules to every CAF secretome (FGF, GM-CSF, Gro $\alpha$ , TGF- $\beta$ , SDF1, HGF, OPN, IL-3 and IL-12p40). When analysis was restricted to cytokines differentially expressed by the CSC and CAF secretomes, there were only 3 cytokines uniquely expressed by the inhibitory CSC secretome, but absent (or produced at very low levels) in the non inhibitory CAF secretome, namely IL-8, IL-12 and VEGF. Among these 3 top overexpressed cytokines, IL-12 does not inhibit T cell proliferation and IFN- $\gamma$  production but instead induces differentiation to IFN- $\gamma$  production. Therefore, IL-8 and VEGF remain as potential candidates of the immunosuppressive activities of the CSC secretome.

#### Intratumoral $\gamma\delta$ T cells correlate with CRC outcome

Previous studies on the prognostic value of tumor-infiltrating  $\gamma\delta$  T cells have shown marked variability, with positive, negative, or even no correlation.<sup>22-23</sup> This is strikingly

depicted by results obtained in CRC in which  $\gamma\delta$  T cells making IL-17 positively correlated with advanced tumor clinicopathologic features in one study,<sup>24</sup> but emerged as the most significant favorable prognostic population in another study.<sup>25</sup>

We initially investigated whether intratumoral  $\gamma\delta$  T cells had clinical relevance, by data mining transcriptomes and clinical files from the larger cohort of  $n = 585$  CRC samples mentioned above. The leucocyte deconvolution of this data set evidenced a link between molecular markers of CRC and their abundance of TILs, whether of the  $\gamma\delta$  or  $\alpha\beta$  TCR subtype. The KRAS mutation status made no difference for these criteria. By contrast, the abundance of both subsets of TILs was significantly higher in mismatch repair-deficient (MMR-D) than -proficient (MMR-P) tumors, in BRAF<sup>mutated</sup> vs. BRAF<sup>wt</sup>, and in TP53<sup>wt</sup> vs. TP53<sup>mutated</sup> tumors. A higher content of TILs was also apparent in tumors positive for the CPG island methylator phenotype (CIMP) vs. their negative counterparts and in tumors negative for the chromosomal instability phenotype (CIN) vs. their positive counterparts. Importantly, each of these prognostic factors influenced in the same direction the abundance of  $\gamma\delta$  TILs and of  $\alpha\beta$  TILs (Fig. 5).

We then correlated frequencies of total  $\gamma\delta$  T cells with clinical outcome by analyzing the independent data set mentioned previously for  $n = 557$  CRC patients for whom follow-up was available. Across the whole cohort, those patients with more

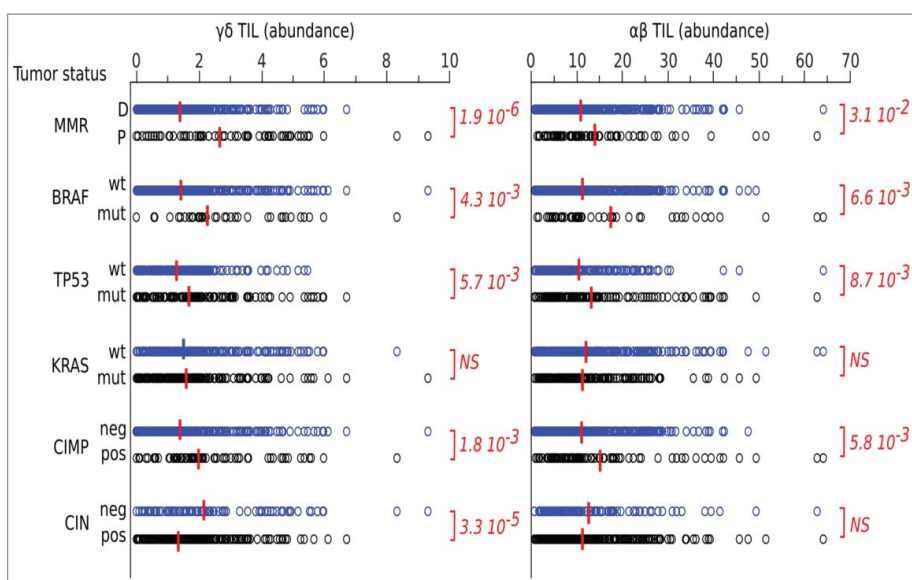


**Figure 5.** Data mining transcriptomes and abundance of TILs. Deconvolution of  $\gamma\delta$  TIL and  $\alpha\beta$  TIL abundances in CRC tumors according to their molecular and clinical hallmarks. Red bar indicate group means. Student's *p* values (2-sided) are indicated.

abundant  $\gamma\delta$  TILs had a better DFS, as confirmed by stratifying patients according to expression of the *TCRGV9*-encoding gene. Patients with higher expression of *IFNG* also presented a higher DFS, whereas those with higher expression of *IL17A* had significantly reduced DFS. This  $\gamma\delta$  TIL and *IFNG*-dependent favorable pattern was conserved when reducing the whole cohort to those patients without lymph node invasion. By contrast, the *IL17*-dependent unfavorable pattern was rather observed in patients with invaded lymph nodes (Fig. 6a). Hence, stratifying the entire cohort according to both  $\gamma\delta$  TIL abundance and *IFNG* expression produced groups with strikingly different DFS, and demonstrated most notably that  $\gamma\delta$  TIL abundance overweighted *IFNG* expression in contributing to this outcome. The same conclusions hold true for  $\gamma\delta$  TIL abundance with regard to *IL17A* expression (Fig. 6b).

## Discussion

Accumulating evidences that high densities of mature T cells, particularly with a Th1 and cytotoxic orientation, in different locations of a primary tumor, correlate with favorable prognosis both in terms of disease-free and overall survival, strongly support the fact that a natural immune reaction controls tumor cell growth and smoothens cancer aggressiveness.<sup>10-11,32</sup> The presence of tumor infiltrating lymphocytes in CRC is associated with a favorable prognosis but is not sufficient to overcome inhibitory changes within the tumor microenvironment over a prolonged period of time. Migration of lymphocytes from the circulation to the tumor site implies that the host immune system is capable of initiating an anti-tumor response. Unfortunately, changes that occur as a result of mutations within tumor cells eventually create an immunosuppressive tumor microenvironment that prevents tumor eradication by TILs.<sup>33-34</sup>

Tumor immunoevasion mechanisms are common and include the downregulation of tumor associated antigens, of MHC, and of costimulatory molecules. By contrast to  $\alpha\beta$  T

cells,  $\gamma\delta$  T cells are not MHC restricted and show less dependence on costimulators such as CD28. Moreover,  $\gamma\delta$  T cells in humans display potent MHC unrestricted cytotoxic activity *in vitro* against various tumors and for example they are fully capable to kill colon cancer stem cells that had been sensitized *in vitro* by zoledronate or low dose chemotherapy.<sup>35-37</sup>

In this paper, we have studied CRC-infiltrating  $\gamma\delta$  T cells and correlated their levels with clinical outcome. Moreover, we have studied the influence of the tumor microenvironment on the functional responses of  $\gamma\delta$  T cells.

Results herewith reported show that  $\gamma\delta$  T cells are present among intratumoral leukocytes but they are a minor T cell population accounting for approximately 20% of total CD3<sup>+</sup> cells. Immunofluorescence analysis additional revealed that  $\gamma\delta$  T cells were mainly detected in the tumor border/stroma, but very rarely in the intratumor tissue.

T cells expressing V $\delta$ 1 were the dominant  $\gamma\delta$  subset in CRC tissue and also in adjacent normal tissues, but V $\delta$ 1 and V $\delta$ 2 T cell subsets were not significantly increased in tumor tissue. Phenotypic analysis showed that most of CRC-infiltrating V $\delta$ 1 and V $\delta$ 2 T cells had T<sub>EM</sub> and T<sub>EMRA</sub> phenotypes, similar to the phenotype of V $\delta$ 1 and V $\delta$ 2 T cells residing in adjacent normal colon tissue, but distinct from that of the corresponding cells from the peripheral blood, suggesting that residence in a non-lymphoid peripheral tissue, regardless of whether it is normal or has undergone tumor transformation, may be a major determinant of the phenotypic characteristics of tumor and tissue  $\gamma\delta$  T cells.

Functional analysis of tumor-infiltrating  $\gamma\delta$  T cells demonstrate that both V $\delta$ 1 and V $\delta$ 2 T cells in CRC and adjacent normal tissues preferentially produce IFN- $\gamma$ , but very low IL-17. Moreover, IFN- $\gamma$  production by both V $\delta$ 1 and V $\delta$ 2 T cells is significantly reduced in CRC tissues, as compared with adjacent normal colon tissue samples. These findings are surprising in light of a previous study showing that  $\gamma\delta$  T cells are the major cellular source of IL-17 in human CRC.<sup>26</sup> Using 3 different FACS gating strategies we were able to confirm the majority of



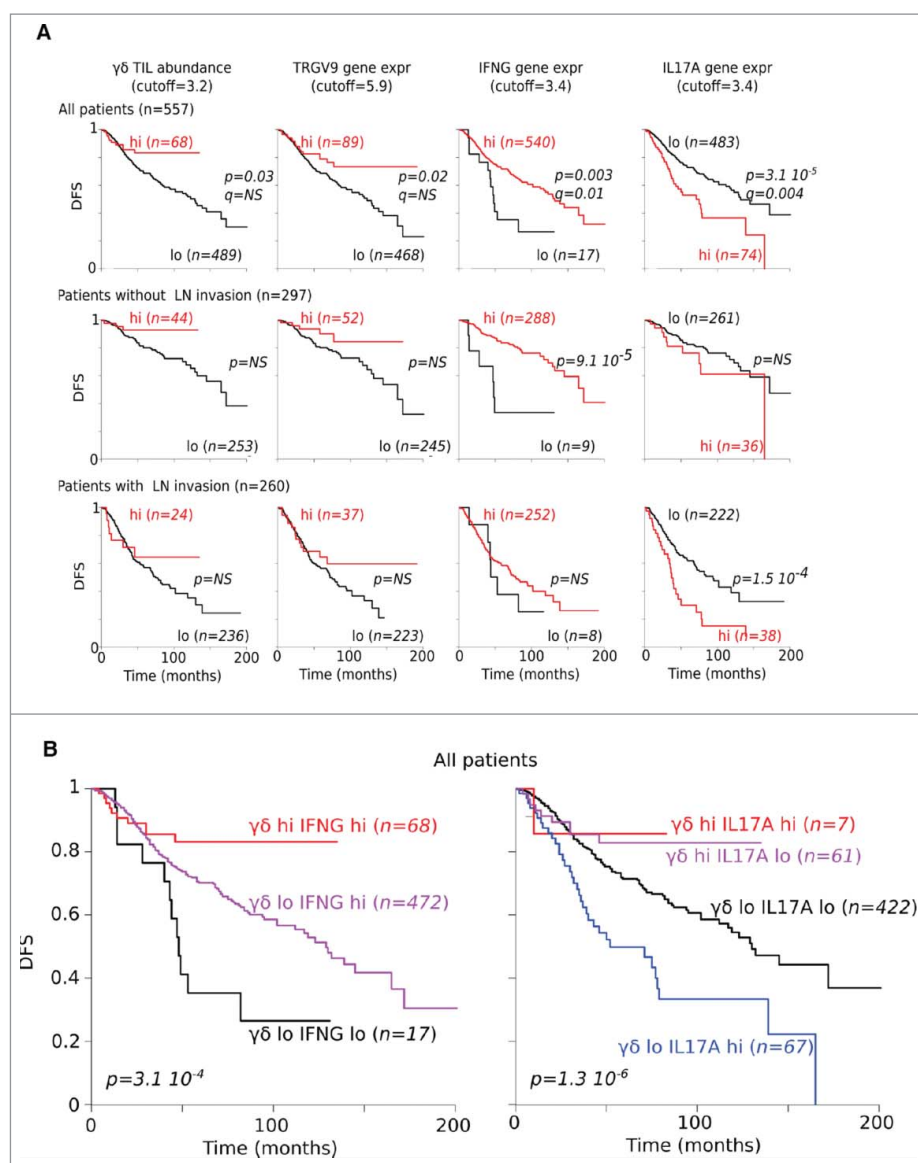


**Figure 6.** Correlation between gene expression and DFS. (A) DFS of CRC patients according to abundance of  $\gamma\delta$  TILs as well as of *TRGV9*, *IFNG* and *IL17A* gene expression levels. (B) DFS of CRC patients according to  $\gamma\delta$  TILs abundance and *IFNG* or *IL17A* gene expression.

IL-17-producing leukocytes both in CRC and in adjacent normal tissues were in fact CD3<sup>+</sup> but not V $\delta$ 1 or V $\delta$ 2, suggesting they are Th17 or Tc17  $\alpha\beta$  T cells, and a sizeable fraction of IL-17 was expressed by CD3<sup>-</sup> cells, probably corresponding to ILC3. We also demonstrated that CD3<sup>+</sup> but V $\delta$ 1<sup>-</sup> and V $\delta$ 2<sup>-</sup> T cells were the major source of TNF- $\alpha$  and IFN- $\gamma$  in both CRC and adjacent normal tissues.

Current data on the prognostic value of CRC-infiltrating  $\gamma\delta$  T cells show marked variability: while one initial study found that  $\gamma\delta$ 17 T cells (expressing either V $\delta$ 1 or V $\delta$ 2) positively correlate with advanced tumor clinicopathologic features,<sup>26</sup> 2 most recent studies<sup>27,31</sup> of expression signature from CRC with overall survival outcomes, revealed intratumoral  $\gamma\delta$  cells,<sup>27</sup> and particularly the V $\gamma$ 9V $\delta$ 2 subset,<sup>31</sup> as the most significant favorable prognostic immune population. Results of data mining transcriptomes and clinical files from a large cohort of CRC samples revealed that 5-year DFS probability was significantly higher in CRC patients with high number of tumor infiltrating  $\gamma\delta$  T cells and IFN- $\gamma$  positive cells.

Thus, it is the maintenance of IFN- $\gamma$  production, that positively associates with better patient outcome, and it is largely influenced by the tumor microenvironment. Accordingly, supernatants from colon CSCs significantly inhibited proliferation and IFN- $\gamma$  production by  $\gamma\delta$  T cells and promoted production of IL-17. Supernatants from other components of the tumor tissue microenvironment such as CAF had limited suppressive ability and did not promote production of IL-17. We also found that colon CSC supernatants significantly inhibited IFN- $\gamma$  production by both CD4 and CD8 T cells, clearly indicating that inhibitory molecules produced by colon CSC have a profound effect on several components of both adaptive ( $\alpha\beta$ ) and innate-like ( $\gamma\delta$ ) T cell immune response. We do not have clear evidence on which molecule(s) is made by colon CSC which is responsible for their immunosuppressive activities: there were only 3 cytokines differentially expressed by the inhibitory CSC secretome, but absent in the non inhibitory CAF secretome, namely IL-8, IL-12 and VEGF. IL-12 does not have

inhibitory activity on T cell proliferation and IFN- $\gamma$  production, which leaves IL-8 and VEGF as potential candidates of the immunosuppressive activities of the colon CSC secretome. While both these 2 molecules have the capability to suppress T cell responses, this is not due to a direct on T cells but is rather mediated by other cell types like dendritic cells, myeloid-derived suppressor cells, M2 macrophages and Treg cells.<sup>38-39</sup> Additionally, it is also possible that immunosuppressive elements like prostaglandins,<sup>40</sup> kynurensins<sup>41</sup> or potassium<sup>42</sup> may be responsible. Therefore, additional studies are needed to find out the molecule responsible for the immunosuppressive activities of the colon CSC secretome on  $\alpha\beta$  and  $\gamma\delta$  T cells.

In conclusion, our results clearly show that  $\gamma\delta$  T cells are a minor population among colon cancer-infiltrating leukocytes, have an effector phenotype but reduced capacity to produce IFN- $\gamma$ , when compared with  $\gamma\delta$  T cells from adjacent normal colon tissue and peripheral blood, but do not produce IL-17. Moreover, they are correlated with clinical outcome indicating they are probably involved in controlling tumor growth at a early stage of disease.

## Materials and methods

### Characteristics of sample cohort

Colon cancer tissues and adjacent normal colon tissues were obtained from the Department of Surgery at the University Hospital of Palermo. We enrolled 70 patients (52 males, 18 females, median age 62 years, age range 42–82 years) undergoing a colon resection for colon adenocarcinoma and diagnosis of CRC was histologically confirmed.

A blood drawing was taken before the surgical excision. The study received authorisation by the local ethical committee and was performed in accordance to the principles of the Helsinki declaration. All individuals gave written informed consent to participate.

### Isolation of tumor-infiltrating and circulating immune cells and flow cytometry analysis

Colon cancer specimens and adjacent normal colon tissues were freshly obtained at the time of primary surgery and transported to the laboratory for processing. Tissue was minced into small pieces followed digestion with Collagenase type IV and DNase (Sigma, St Louis, MO) for 2 hrs at 37°C 5% CO<sub>2</sub>. After digestion, the cells extracted were washed twice in incomplete medium (RPMI 1640, Gibco, Grand Island, NY). Whole blood samples were obtained from the same patients recruited for the collection of tissue specimens before the surgical procedure, and used for the comparative analysis between peripheral blood and cancer tissue. The peripheral blood mononuclear cells (PBMCs) were separated from whole blood by density gradient centrifugation using Ficoll-Hypaque (Pharmacia Biotech, Uppsala, Sweden).

Both PBMC and tumor infiltrating cells were stained for live/dead discrimination using Invitrogen Live/Dead fixable violet dead cell stain kit (Invitrogen, Carlsbad, CA). Fc receptor

blocking was performed with human immunoglobulin (Sigma, 3  $\mu$ g/ml final concentration) followed by surface staining with different fluorochrome-conjugated antibodies to study the composition of the different subpopulations. The fluorescein isothiocyanate (FITC)-, phycoerythrin (PE)-, PE-Cy5-, allophycocyanin (APC)-, phycoerythrin-Cy7 (PECy7)-, allophycocyanin-Cy7 (APC-Cy7)-conjugated monoclonal antibodies (mAbs) used to characterize the entire population were the following: anti-CD3 (Cat 45–0037 eBioscience, Cat 300412 and Cat 300420 Biolegend), anti-CD45 (Cat 560274 BD Bioscience), anti-pan  $\gamma\delta$  TCR (Cat 555717 BD), anti-V $\delta$ 1 (Cat PG196007 ThermoFisher), anti-V $\delta$ 2 (Cat 331408 Biolegend), anti-CD4, (Cat 17–0279 eBioscience), anti-CD45RA (Cat 25–0458 eBioscience), anti-CD19 (Cat 302228 Biolegend), anti-CD4, (Cat 130–094–158 Miltenyi, Cat 348809 BD), anti CD8 (Cat 555367 BD) and anti-CD56 (Cat 341027 BD).

Expression of surface markers was determined by flow cytometry on a FACSCanto II Flow Cytometer with the use of the FlowJo software (BD Biosciences). The gating strategy involved progressively measuring total cells; viable cells only; lymphomonocytes and specific cell types. For every sample 100.000 nucleated cells were acquired and values are expressed as percentage of viable lymphomonocytes, as gated by forward and side scatter.

To study intracellular IFN- $\gamma$ , IL-17 and TNF- $\alpha$ , cells from tumor and adjacent normal colon tissues were stimulated with Ionomycin and PMA in the presence of monensin for 4 hrs at 37°C in 5% CO<sub>2</sub>. The cells were harvested, washed twice in PBS with 1% FCS and fixed with PBS containing 4% paraformaldehyde overnight at 4°C. Fixation was followed by permeabilization with PBS containing 1% FCS, 0.3% saponin, and 0.1% Na azide for 15 min at 4°C. Staining of intracellular cytokines was performed by incubation of fixed permeabilized cells with FITC-labeled anti-IFN- $\gamma$  (Cat 502506 Biolegend), APC-labeled anti-IL-17A (Cat 130–096–748 Miltenyi) and PeVio770 anti-TNF- $\alpha$  (Cat 130–096–748 Miltenyi). After 2 more washes in PBS containing 1% FCS, the cells were analyzed by FACS Canto II flow cytometer (BD Bioscience). Viable lymphocytes were gated by forward and side scatter, and analysis was performed on 100,000 acquired events for each sample by using FlowJo and the following gating strategy to detect lymphocytes from FSC/SSC, single cells, double positive CD45<sup>+</sup> CD3<sup>+</sup>, and V $\delta$ 1 and V $\delta$ 2 positive T cells.

Polyclonal  $\gamma\delta$  T cell lines were prepared as described previously,<sup>43-44</sup> were labeled with CFSE (Molecular Probes, Eugene, USA) and  $5 \times 10^5$  cells were incubated with CAF and CSC supernatants in 24-well plates (Costar, Cambridge, MA) for 7 d at 37°C, 5% CO<sub>2</sub>, in addition to PHA or anti CD3/CD28. Proliferation was assessed after 7 d of culture according to loss of CFSE labeling.

To obtain CD4 and CD8 polyclonal  $\alpha\beta$  T cell lines, CD4 and CD8 T cells were sorted from PBMC of healthy donors using MACS cell separation kit, and incubated for 2 weeks with PHA, IL-2 and Beads (Dynabeads, ThermoFisher). Cell lines were incubated with CAF and CSC supernatants for 48 hrs and then stained for IL-17 and IFN- $\gamma$  content upon Ionomycin and PMA stimulation.

## Preparation of CAF and CSC conditioned medium, Luminex and ELISA analysis

Primary cancer associated fibroblasts (CAFs) and colon cancer stem cells (CSCs) were obtained from 15 surgical resection of CRC subjected to mechanical and enzymatic digestion with collagenase (0.6 mg/ml, Gibco) and hyaluronidase (10  $\mu$ g/ml, Sigma). Cell suspension was cultured in 10% fetal bovine serum (FBS) Dulbecco's modified Eagle's medium (DMEM) in adhesion flasks, to obtain CAFs, or in low-adhesion conditions and in serum-free medium supplemented with EGF and  $\beta$ -FGF, which allows the selective growth of colon CSCs.<sup>45-46</sup> Cells were plated and incubated in their specific medium for 48 hrs; the medium was then collected and used for luminex assay.

Fourthly-eight cytokines (IL-1 $\alpha$ , IL-1 $\beta$ , IL-1R antagonist, IL-2, IL-2R $\alpha$ , IL-3, IL-4, IL-5, IL-6, IL-7, IL-9, IL-10, IL-12, IL-12 (p40), IL-13, IL-15, IL-16, IL-17, IL-18, TNF- $\alpha$ , TNF- $\beta$ , IFN- $\alpha_2$ , IFN- $\gamma$ , G-CSF, GM-CSF, M-CSF, FGF- $\beta$ , VEGF, PDGF, MIF, MIG, HGF, LIF, NGF- $\beta$ , SCF, SCGF- $\beta$ , SDF-1 $\alpha$ , TRAIL, Eotaxin, IP-10, IL-8, MIP-1 $\alpha$ , MIP-1 $\beta$ , MCP-1, RANTES, CTACK, GRO- $\alpha$ , MCP-3) were analyzed in CAF and CSC conditioned medium by xMAP multiplex technology on the Luminex platform (Luminex, Austin, TX), using Bio-Rad reagents (Bio-Plex Pro<sup>TM</sup> Human Cytokine 27-plex Assay #M500KCAF0Y and Bio-Plex Pro<sup>TM</sup> Human Cytokine 21-plex Assay #MF0005KMII, Bio-Rad, Hercules, CA) acquired and analyzed with the Bioplex Manager Software (Bio-Rad). Responses were scored positive if the value was 2-fold over the negative control. TGF- $\beta$  and OPN were measured by ELISA according to the manufacturer's instructions (R&D Systems).<sup>46</sup>

## Immunofluorescence analysis

Fresh frozen tissue samples were incubated with primary antibodies to the pan- $\gamma\delta$  TCR and CD3 and in a subsequent secondary step, FITC-conjugated goat anti-rabbit and Rhodamine B200-conjugated goat anti-mouse IgG were used to detect them. Irrelevant isotype-matched primary mAbs were used to control for nonspecific staining. Analysis was performed with a confocal laser scanning microscopy equipped with 20x, 40x and 63x objectives. The tumor border configuration was diagnosed according to the method proposed by Jass et al.<sup>47</sup> at low magnification. Briefly, the tumor margins were identified as infiltrating when there was no recognizable margin of growth and a "streaming dissection" between the normal structures of the bowel wall was present. Margins were considered pushing when they were reasonably well circumscribed, and they often were associated with a well-developed inflammatory lamina.

## Transcriptome analysis

Public raw data of 585 colon cancers transcriptomes using Affymetrix HGU133 Plus 2.0 microarrays were downloaded from the NCBI-GEO data set repository (GSE39582<sup>29</sup>, <https://www.ncbi.nlm.nih.gov/geo>), normalized together and collapsed to HUGO gene symbols using chipset definition files available from the NCBI gene expression omnibus. The Pearson correlation coefficient between *IFNG*, *IL17A*, *TRGV9* and *CD3D* gene expressions were calculated.

Deconvolution of immune population are calculated using the CIBERSORT software with 500 Monte Carlo iterations<sup>30</sup> (<https://cibersort.stanford.edu/>) associated with the LM7 matrix.<sup>31</sup> Sample Enrichment Scores (SES)<sup>48</sup> of immune genes were computed using the open source software AutoCompare-SES ([https://sites.google.com/site/fredsoftwares/products/auto\\_compare\\_ses](https://sites.google.com/site/fredsoftwares/products/auto_compare_ses)) with normalized settings.  $\alpha\beta$  and  $\gamma\delta$  TIL abundance were automatically calculated from the deconvolution result and SES using the open source software DeepTIL (<https://sites.google.com/site/fredsoftwares/products/deeptil>).<sup>31</sup>

## SPADE analysis

Spanning-tree progression analysis of density-normalized events (SPADE)<sup>49</sup> clustering algorithm on the Cytobank.org platform was performed to visualize single cells, among live CD45<sup>+</sup> lymphocytes from 6 subjects. The nodes of the tree reproduce clusters of cells that are similar in marker expression. SPADE uses the size and color of each node to signify the number of cells and median marker expression, respectively.

## Statistics

Data were analyzed for statistical significance using Mann-Whitney test for 2 groups and Kruskal-Wallis test for more than 2 groups. Differences between groups with a probability of  $\leq 0.05$  were regarded as significant. All data were analyzed using GraphPad Prism version 6.0e (GraphPad, San Diego, CA). All values are expressed as mean  $\pm$  SD. Comparison of TIL abundance in clinical groups were done using unpaired Student t-test.

For Kaplan-Meier plots, optimal cutoffs were determined with the survival R package<sup>50</sup> and the Log-Rank *p* values were corrected using the Benjamini-Hochberg method.<sup>51</sup>

## Disclosure of potential conflicts of interest

No potential conflicts of interest were disclosed.

## Acknowledgments

We would like to thank Achim Jungbluth, Department of Pathology Memorial Sloan-Kettering Cancer Center New York, for helping with immunofluorescence analysis of colon cancer tissue samples and Adrian Hayday for reading the manuscript and for training Elena Lo Presti at King's College London.

## Funding

This work was supported in part by grants from the Ministry of Health "Ricerca Finalizzata 2007" to F.D and by Associazione Italiana per la Ricerca sul Cancro (AIRC) to M.T. (AIRC IG 14415).

## ORCID

M. Tosolini  <http://orcid.org/0000-0001-5278-5952>  
J. J. Fourniè  <http://orcid.org/0000-0001-6542-6908>

## References

- Cunningham D, Atkin W, Lenz HJ, Lynch HT, Minsky B, Nordlinger B, Starling N. Colorectal cancer. *Lancet* 2010; 375(9719):1030-47; PMID:20304247; [https://doi.org/10.1016/S0140-6736\(10\)60353-4](https://doi.org/10.1016/S0140-6736(10)60353-4)
- Aune D, Lau R, Chan DS, Vieira R, Greenwood DC, Kampman E, Norat T. Dairy products and colorectal cancer risk: A systematic review and meta-analysis of cohort studies. *Ann Oncol* 2012; 23(1):37-45; PMID:21617020; <https://doi.org/10.1093/annonc/mdr269>
- Kennedy DA, Stern SJ, Moretti M, Matok I, Sarkar M, Nickel C, Koren G. Folate intake and the risk of colorectal cancer: A systematic review and meta-analysis. *Cancer Epidemiol* 2011; 35(1):2-10; PMID:21177150; <https://doi.org/10.1016/j.canep.2010.11.004>
- Ma Y, Zhang P, Wang F, Yang J, Liu Z, Qin H. Association between vitamin D and risk of colorectal cancer: A systematic review of prospective studies. *J Clin Oncol* 2011; 29(28):3775-82; PMID:21876081; <https://doi.org/10.1200/JCO.2011.35.7566>
- Jasperson KW, Tuohy TM, Neklason DW, Burt RW. Hereditary and familial colon cancer. *Gastroenterology* 2010; 138(6):2044-58; PMID:20420945; <https://doi.org/10.1053/j.gastro.2010.01.054>
- Coussens LM, Werb Z. Inflammation and cancer. *Nature* 2002; 420:860-7; PMID:12490959; <https://doi.org/10.1038/nature01322>
- Hannahan D, Weinberg RA. Hallmarks of cancer: The next generation. *Cell* 2011; 144(5):646-74; PMID:21376230; <https://doi.org/10.1016/j.cell.2011.02.013>
- Fridman WH, Dieu-Nosjean MC, Pagès F, Cremer I, Damotte D, Sautès-Fridman C, Galon J. The immune microenvironment of human tumors: General significance and clinical impact. *Cancer Microenviron* 2013; 6(2):117-22; PMID:23108700; <https://doi.org/10.1007/s12307-012-0124-9>
- Sasada T, Suekane S. Variation of tumor-infiltrating lymphocytes in human cancers: Controversy on clinical significance. *Immunotherapy* 2011; 3(10):1235-51; PMID:21995574; <https://doi.org/10.2217/imt.11.106>
- Gooden MJ, de Bock GH, Leffers N, Daemen T, Nijman HW. The prognostic influence of tumour-infiltrating lymphocytes in cancer: A systematic review with meta-analysis. *Br J Cancer* 2011; 105(1):93-103; PMID:21629244; <https://doi.org/10.1038/bjc.2011.189>
- Galon J, Costes A, Sanchez-Cabo F, Kirilovsky A, Mlecnik B, Lagorce-Pagès C, Tosolini M, Camus M, Berger A, Wind P, et al. Type, density, and location of immune cells within human colorectal tumors predicts clinical outcome. *Science* 2006; 313(5795):1960-4; PMID:17008531; <https://doi.org/10.1126/science.1129139>
- Pagès F, Kirilovsky A, Mlecnik B, Asslaber M, Tosolini M, Bindea G, Lagorce C, Wind P, Marliot F, Bruneval P, et al. In situ cytotoxic and memory T cells predict outcome in early-stage colorectal cancer patients. *J Clin Oncol* 2009; 27(35):5944-51; PMID:19858404; <https://doi.org/10.1200/JCO.2008.19.6147>
- Groh V, Porcelli S, Fabbri M, Lanier LL, Picker LJ, Anderson T, Warnke RA, Bhan AK, Strominger JL, Brenner MB. Human lymphocytes bearing T cell receptor  $\gamma\delta$  are phenotypically diverse and evenly distributed throughout the lymphoid system. *J Exp Med* 1989; 169(4):1277-94; PMID:2564416; <https://doi.org/10.1084/jem.169.4.1277>
- Bonneville M, O'Brien RL, Born WK.  $\gamma\delta$  T cell effector functions: A blend of innate programming and acquired plasticity. *Nat Rev Immunol* 2010; 10(7):467-78; PMID:20539306; <https://doi.org/10.1038/nri2781>
- Constant P, Davodeau F, Peyrat MA, Poquet Y, Puzo G, Bonneville M, Fournié JJ. Stimulation of human  $\gamma\delta$  T cells by nonpeptidic mycobacterial ligands. *Science* 1994; 264(5156):267-70; PMID:8146660; <https://doi.org/10.1126/science.8146660>
- Eberl M, Hintz M, Reichenberg A, Kollas AK, Wiesner J, Jomaa H. Microbial isoprenoid biosynthesis and human  $\gamma\delta$  T cell activation. *FEBS Lett* 2003; 544(1-3):4-10; PMID:12782281; [https://doi.org/10.1016/S0014-5793\(03\)00483-6](https://doi.org/10.1016/S0014-5793(03)00483-6)
- Tanaka Y, Morita CT, Nieves E, Brenner MB, Bloom BR. Natural and synthetic non-peptide antigens recognized by human  $\gamma\delta$  T cells. *Nature* 1995; 375(6527):155-8; PMID:7753173; <https://doi.org/10.1038/375155a0>
- Vavassori S, Kumar A, Wan GS, Ramanjaneyulu GS, Cavallari M, El Daker S, Beddoe T, Theodossis A, Williams NK, Gostick E, et al. Butyrophilin 3A1 binds phosphorylated antigens and stimulates human  $\gamma\delta$  T cells. *Nat Immunol* 2013; 14(9):908-16; PMID:23872678; <https://doi.org/10.1038/ni.2665>
- Harly C, Guillaume Y, Nedellec S, Peigné CM, Mönkkönen H, Mönkkönen J, Li J, Kuball J, Adams EJ, Netzer S, et al. Key implication of CD277/butyrophilin-3 (BTN3A) in cellular stress sensing by a major human  $\gamma\delta$ T-cell subset. *Blood* 2012; 120(11):2269-79; PMID:22767497; <https://doi.org/10.1182/blood-2012-05-430470>
- Sandstrom A, Peigné CM, Léger A, Crooks JE, Konczak F, Gesnel MC, Breathnach R, Bonneville M, Scotet E, Adams EJ. The intracellular B30.2 domain of butyrophilin 3A1 binds phosphoantigens to mediate activation of human V $\gamma$ 9V $\delta$ 2 T cells. *Immunology* 2014; 40(4):490-500; PMID:24703779; <https://doi.org/10.1016/j.immuni.2014.03.003>
- Gober H, Kistowska M, Angman L, Jenö P, Mori L, De Libero G. Human T cell receptor  $\gamma\delta$  cells recognize endogenous mevalonate metabolites in tumor cells. *J Exp Med* 2003; 197(2):163-8; PMID:12538656; <https://doi.org/10.1084/jem.20021500>
- Dieli F, Gebbia N, Poccia F, Caccamo N, Montesano C, Fulfaro F, Arcara C, Valerio MR, Meraviglia S, Di Sano C, et al. Induction of  $\gamma\delta$  T lymphocyte effector functions by bisphosphonate zoledronic acid in cancer patients in vivo. *Blood* 2003; 102(6):2310-1; PMID:12959943; <https://doi.org/10.1182/blood-2003-05-1655>
- Dieli F, Poccia F, Lipp M, Sireci G, Caccamo N, Di Sano C, Salerno A. Differentiation of effector/memory V $\delta$ 2 T cells and migratory routes in lymph nodes or inflammatory sites. *J Exp Med* 2003; 198(3):391-7; PMID:12900516; <https://doi.org/10.1084/jem.20030235>
- Lo Presti E, Dieli F, Meraviglia S. Tumor-infiltrating  $\gamma\delta$  T lymphocytes: Pathogenic role, clinical significance, and differential programming in the tumor microenvironment. *Front Immunol* 2014; 5:607; PMID:25505472; <https://doi.org/10.3389/fimmu.2014.00607>
- Silva-Santos B, Serre K, Norell H.  $\gamma\delta$ T cells in cancer. *Nat Rev Immunol* 2015; 15(11):683-91; PMID:26449179; <https://doi.org/10.1038/nri3904>
- Wu P, Wu D, Ni C, Ye J, Chen W, Hu G, Wang Z, Wang C, Zhang Z, Xia W, et al.  $\gamma\delta$ T17 cells promote the accumulation and expansion of myeloid-derived suppressor cells in human colorectal cancer. *Immununity* 2014; 40:785-800; PMID:24816404; <https://doi.org/10.1016/j.immuni.2014.03.013>
- Gentles AJ, Newman AM, Liu CL, Bratman SV, Feng W, Kim D, Nair VS, Xu Y, Khuong A, Hoang CD, et al. The prognostic landscape of genes and infiltrating immune cells across human cancers. *Nat Med* 2015; 21(8):938-45; PMID:26193342; <https://doi.org/10.1038/nm.3909>
- Marisa L, Reyniès LA, Duval A, Selves J, Gaub MP, Vescovo L, Etienne-Grimaldi MC, Schiappa R, Guenot D, Ayadi M, et al. Gene expression classification of colon cancer into molecular subtypes: characterization, validation, and prognostic value. *PLoS Med* 2013; 10:e1001453; PMID:23700391; <https://doi.org/10.1371/journal.pmed.1001453>
- GSE39582, <https://www.ncbi.nlm.nih.gov/geo>.
- Newman AM, Liu CL, Green MR, Gentles AJ, Feng W, Xu Y, Hoang CD, Diehn M, Alizadeh AA. Robust enumeration of cell subsets from tissue expression profiles. *Nat Meth* 2015; 12:453-7; PMID:25822800; <https://doi.org/10.1038/nmeth.3337>
- Tosolini M, Pont F, Poupot M, Vergez F, Nicolau-Travers ML, Vermijlen D, Sarry JE, Dieli F, Fournie JJ. Assessment of tumor-infiltrating TCRV $\gamma$ 9V $\delta$ 2 lymphocyte abundance by deconvolution of human cancers microarrays. *Oncoimmunology* 2017; 6:e1284723; PMID:28405516; <https://doi.org/10.1080/2162402X.2017.1284723>
- Smyth MJ, Dunn GP, Schreiber RD. Cancer immunosurveillance and immunoediting: The roles of immunity in suppressing tumor development and shaping tumor immunogenicity. *Adv Immunol* 2006; 90:1-50; PMID:16730260; [https://doi.org/10.1016/S0065-2776\(06\)90001-7](https://doi.org/10.1016/S0065-2776(06)90001-7)
- Fridman WH, Pagès F, Sautès-Fridman C, Galon J. The immune contexture in human tumours: Impact on clinical outcome. *Nat Rev Cancer* 2012; 12(4):298-306; PMID:22419253; <https://doi.org/10.1038/nrc3245>
- Gajewski TF, Schreiber H, Fu YX. Innate and adaptive immune cells in the tumor microenvironment. *Nat Immunol* 2013; 14:1014-22; PMID:24048123; <https://doi.org/10.1038/ni.2703>
- Todaro M, D'Asaro M, Caccamo N, Iovino F, Francipane MG, Meraviglia S, Orlando V, La Mendola C, Gulotta G, Salerno A, et al.

- Efficient killing of human colon cancer stem cells by  $\gamma\delta$  T lymphocytes. *J Immunol* 2009; 182(11):7287-96; PMID:19454726; <https://doi.org/10.4049/jimmunol.0804288>
36. Todaro M, Orlando V, Cicero G, Caccamo N, Meraviglia S, Stassi G, Dieli F. Chemotherapy sensitizes colon cancer initiating cells to  $V\gamma 9V\delta 2$  T cell-mediated cytotoxicity. *PLoS One* 2013; 8(6):e65145; PMID:23762301; <https://doi.org/10.1371/journal.pone.0065145>
  37. Todaro M, Meraviglia S, Caccamo N, Stassi G, Dieli F. Combining conventional chemotherapy and  $\gamma\delta$  T cell-based immunotherapy to target cancer-initiating cells. *Oncoimmunology* 2013; 2(9):e25821; PMID:24244907; <https://doi.org/10.4161/onci.25821>
  38. Liu Q, Li A, Tian Y, Wu JD, Liu Y, Li T, Chen Y, Han Y, Wu K. The CXCL8-CXCR1/2 pathways in cancer. *Cytokine Growth Factor Rev* 2016; 31:61-71; PMID:27578214; <https://doi.org/10.1016/j.cytogfr.2016.08.002>
  39. Voron T, Marcheteau E, Pernot S, Colussi O, Tartour E, Taieb J, Terme M. Control of the immune response by pro-angiogenic factors. *Front Oncol* 2014; 4:70; PMID:24765614; <https://doi.org/10.3389/fonc.2014.00070>
  40. Basingab FS, Ahmadi M, Morgan DJ. IFN- $\gamma$ -dependent interactions between ICAM-1 and LFA-1 counteract prostaglandin E2-mediated inhibition of antitumor CTL responses. *Cancer Immunol Res* 2016; 4(5):400-11; PMID:26928462; <https://doi.org/10.1158/2326-6066.CCR-15-0146>
  41. Zhai L, Spranger S, Binder DC, Gritsina G, Lauing KL, Giles FJ, Wainwright DA. Molecular pathways: Targeting IDO1 and other tryptophan dioxygenases for cancer immunotherapy. *Clin Cancer Res* 2015; 21(24):5427-33; PMID:26519060; <https://doi.org/10.1158/1078-0432.CCR-15-0420>
  42. Eil R, Vodnala SK, Clever D, Klebanoff CA, Sukumar M, Pan JH, Palmer DC, Gros A, Yamamoto TN, Patel SJ, et al. Ionic immune suppression within the tumour microenvironment limits T cell effector function. *Nature* 2016; 537(7621):539-43; PMID:27626381; <https://doi.org/10.1038/nature19364>
  43. Sireci G, Espinosa E, Di Sano C, Dieli F, Fournié JJ, Salerno A. Differential activation of human  $\gamma\delta$  cells by non peptide phosphoantigens. *Eur J Immunol* 2001; 31(5):1628-35; PMID:11465120; [https://doi.org/10.1002/1521-4141\(200105\)31:5%3c1628::AID-IMMU1628%3e3.0.CO;2-T](https://doi.org/10.1002/1521-4141(200105)31:5%3c1628::AID-IMMU1628%3e3.0.CO;2-T)
  44. Sireci G, Champagne E, Fournié JJ, Dieli F, Salerno A. Patterns of phosphoantigen stimulation of human  $V\gamma 9V\delta 2$  T cell clones include Th0 cytokines. *Hum Immunol* 1997; 58(2):70-82; PMID:9475336; [https://doi.org/10.1016/S0198-8859\(97\)00211-5](https://doi.org/10.1016/S0198-8859(97)00211-5)
  45. Ricci-Vitiani L, Lombardi DG, Pilozzi E, Biffoni M, Todaro M, Peschle C, De Maria R. Identification and expansion of human colon-cancer-initiating cells. *Nature* 2007; 445(7123):111-5; PMID:17122771; <https://doi.org/10.1038/nature05384>
  46. Todaro M, Alea MP, Di Stefano AB, Cammareri P, Vermeulen L, Iovino F, Tripodo C, Russo A, Gulotta G, Medema JP, et al. Colon cancer stem cells dictate tumor growth and resist cell death by production of interleukin-4. *Cell Stem Cell* 2007; 1(4):389-402; PMID:18371377; <https://doi.org/10.1016/j.stem.2007.08.001>
  47. Shinto E, Mochizuki H, Ueno H, Matsubara O, Jass JR. A novel classification of tumour budding in colorectal cancer based on the presence of cytoplasmic pseudo-fragments around budding foci. *Histopathology* 2005; 47(1):25-31; PMID:15982320; <https://doi.org/10.1111/j.1365-2559.2005.02162.x>
  48. Tosolini M, Algans C, Pont F, Ycart B, Fournie JJ. Large scale microarray profiling reveals four stages of immune escape in non-Hodgkin's lymphomas. *Oncoimmunology* 2016; 5(7):e1188246; PMID:27622044; <https://doi.org/10.1080/2162402X.2016.1188246>
  49. Qiu P, Simonds EF, Bendall SC, Gibbs KD Jr, Bruggner RV, Linderman MD, Sachs K, Nolan GP, Plevritis SK. Extracting a cellular hierarchy from high-dimensional cytometry data with SPADE. *Nat Biotechnol* 2011; 29(10):886-91; PMID:21964415; <https://doi.org/10.1038/nbt.1991>
  50. Therneau TM, Grambsch PM. Modeling survival data: Extending the cox model. New York: Springer (2000).
  51. Hochberg Y, Benjamini Y. More powerful procedures for multiple significance testing. *Stat Med* 1990; 9(7):811-8; PMID:2218183; <https://doi.org/10.1002/sim.4780090710>